Redox Biology 37 (2020) 101746

Contents lists available at ScienceDirect

Redox Biology

journal homepage: www.elsevier.com/locate/redox

Copper interferes with selenoprotein synthesis and activity

Maria Schwarz [a,b], Kristina Lossow [a,b,c], Katja Schirl [a], Julian Hackler [b,d], Kostja Renko [d,e], Johannes Florian Kopp [b,f], Tanja Schwerdtle [b,e,f], Lutz Schomburg [b,d], Anna Patricia Kipp [a,b,*]

[a] Department of Molecular Nutritional Physiology, Institute of Nutritional Sciences, Friedrich Schiller University Jena, Jena, 07743, Germany
[b] TraceAge-DFG Research Unit on Interactions of Essential Trace Elements in Healthy and Diseased Elderly, Potsdam-Berlin-Jena, Germany
[c] German Institute of Human Nutrition, Nuthetal, 14558, Germany
[d] Institute for Experimental Endocrinology, Charité - University Medical School Berlin, Berlin, 13353, Germany
[e] German Federal Institute for Risk Assessment (BfR), Berlin, Germany
[f] Department of Food Chemistry, Institute of Nutritional Science, University of Potsdam, Nuthetal, 14558, Germany

ARTICLE INFO

Keywords:
Selenium
Copper
Selenoprotein synthesis
Glutathione peroxidase
Thioredoxin reductase

ABSTRACT

Selenium and copper are essential trace elements for humans, needed for the biosynthesis of enzymes contributing to redox homeostasis and redox-dependent signaling pathways. Selenium is incorporated as selenocysteine into the active site of redox-relevant selenoproteins including glutathione peroxidases (GPX) and thioredoxin reductases (TXNRD). Copper-dependent enzymes mediate electron transfer and other redox reactions. As selenoprotein expression can be modulated e.g. by H_2O_2, we tested the hypothesis that copper status affects selenoprotein expression. To this end, hepatocarcinoma HepG2 cells and mice were exposed to a variable copper and selenium supply in a physiologically relevant concentration range, and transcript and protein expression as well as GPX and TXNRD activities were compared. Copper suppressed selenoprotein mRNA levels of GPX1 and SELENOW, downregulated GPX and TXNRD activities and decreased UGA recoding efficiency in reporter cells. The interfering effects were successfully suppressed by applying the copper chelators bathocuproinedisulfonic acid or tetrathiomolybdate. In mice, a decreased copper supply moderately decreased the copper status and negatively affected hepatic TXNRD activity. We conclude that there is a hitherto unknown interrelationship between copper and selenium status, and that copper negatively affects selenoprotein expression and activity most probably via limiting UGA recoding. This interference may be of physiological relevance during aging, where a particular shift in the selenium to copper ratio has been reported. An increased concentration of copper in face of a downregulated selenoprotein expression may synergize and negatively affect the cellular redox homeostasis contributing to disease processes.

1. Introduction

The biological functions of the essential trace element (TE) selenium (Se) have been attributed primarily to selenoproteins. In the human genome, 25 genes encode for selenoproteins [1]. The best characterized selenoprotein families are the glutathione peroxidases (GPXs), the thioredoxin reductases (TXNRDs), and the deiodinases (DIOs). GPXs and TXNRDs are important modulators of the cellular redox homeostasis by either catalyzing the glutathione (GSH)-dependent reduction of hydroperoxides or NADPH-dependent reduction of thioredoxins and several further substrates, respectively. Selenoprotein P (SelenoP) comprises almost 50% of total plasma Se and transports Se from liver to peripheral tissues [2]. Besides these, the function of several further selenoproteins are still not entirely understood, however, almost all of them appear to be involved in maintaining the cellular redox homeostasis. This holds especially true for selenoproteins such as selenoprotein H (SelenoH) and SelenoW which contain selenocysteine (Sec) as part of a CXXU motif, indicating that they are putative oxidoreductases. In addition, SelenoW has been shown to act in an antioxidant manner after its glutathionylation [3]. During selenoprotein synthesis, Se is cotranslationally incorporated as Sec which is encoded by the base triplet UGA. The specific Sec $tRNA^{[Ser]Sec}$ becomes first aminoacylated with serine which is phosphorylated, accordingly. Both steps are catalyzed by seryl-tRNA synthetase (SERS) and O-phosphoseryl-tRNA kinase (PSTK), respectively. The selenophosphate synthetase 2 (SEPHS2), which also belongs

* Corresponding author. Department of Molecular Nutritional Physiology, Institute of Nutritional Sciences, Friedrich Schiller University Jena, Dornburger Str. 24, 07743 Jena, Germany.
E-mail address: anna.kipp@uni-jena.de (A.P. Kipp).

https://doi.org/10.1016/j.redox.2020.101746
Received 4 September 2020; Received in revised form 1 October 2020; Accepted 4 October 2020
Available online 7 October 2020

Abbreviations

Atox1	antioxidant protein 1
BCS	bathocuproinedisulfonic acid
BSO	buthionine-sulfoximine
CCS	Cu chaperone for superoxide dismutase 1
Ctr1	Cu transporter 1
Cu	copper
DIO	deiodinase
DMT1	divalent metal-ion transporter 1
DTNB	5,5′-dithio-bis-(2-nitrobenzoic acid)
eEFSec	Sec-specific translation elongation factor
GCL	glutamate-cysteine ligase
GSH	glutathione
GR	glutathione reductase
MT	metallothionein
MTF-1	metal regulatory transcription factor 1
MTT	thiazolyl blue tetrazolium bromide
NQO1	NAD(P)H quinone dehydrogenase 1
Nrf2	nuclear factor erythroid 2 p45-related factor 2
PSTK	O-phosphoseryl-tRNA kinase
RT	room temperature
Se	selenium
Sec	selenocysteine
SECIS	Sec insertion sequence
SeMet	selenomethionine
Sephys2	selenophosphate synthetase 2
SepSecs	Sep (O-phosphoserine) tRNA:Sec tRNA synthase
SerS	seryl-tRNA synthetase
SOD1	superoxide dismutase 1
TE	trace element
TNB	2-nitro-5-thiobenzoic acid
TTM	tetrathiomolybdate
TXRF	total reflection X-ray fluorescence

to the group of selenoproteins generates monoselenophosphate, which is then used by Sep (O-phosphoserine) tRNA:Sec tRNA synthase (SEPSECS) to form selenocysteyl-tRNA$^{[Ser]Sec}$. To initiate Sec incorporation rather than termination of protein synthesis, selenoprotein mRNAs contain a special Sec insertion sequence (SECIS) element in their 3' untranslated region. For efficient translation of UGA to Sec, additional factors such as the Sec-specific translation elongation factor (EEFSEC) are needed (overview in Ref. [2]).

The selenoprotein synthesis can be modulated at different levels. The best characterized principle is based on the efficiency of Sec incorporation affecting selenoprotein synthesis mainly at the translational level. In case of Se deficiency, expression levels of favored selenoproteins, namely housekeeping selenoproteins such as TXNRD1, TXNRD2, and GPX4 are maintained while expression levels of so-called stress-responsive selenoproteins e.g. GPX1, SELENOH, and SELENOW are rapidly decreased. This is also called hierarchy of selenoproteins [2]. In addition, drugs such as the aminoglycoside geneticin (G418) can induce misinterpretation of the UGA codon, primarily under Se deficiency, leading to increased rates of dysfunctional variants of selenoproteins [4–6]. Besides the translational regulation, selenoprotein expression can be additionally modulated at the transcriptional level. A prominent example relates to the activation of nuclear factor erythroid 2 p45-related factor 2 (Nrf2) by sulforaphane, positively affecting GPX2 and TXNRD1 expression [7,8]. Besides sulforaphane, e.g. hydroperoxides contribute to selenoprotein expression and modulate read-through efficiency [9]. These examples indicate that redox-responsive transcription factors and the cellular redox homeostasis synergistically affect selenoprotein expression at different molecular levels.

Besides factors that directly impact the cellular redox homeostasis, other mechanisms may contribute in a more indirect manner. This includes the essential TE copper (Cu), which is a cofactor of antioxidant enzymes such as superoxide dismutase 1 (SOD1) [10], but at higher concentrations could also contribute as free ion to the generation of reactive oxygen species [11]. Furthermore, Cu is able to oxidize free thiol groups and to modulate the cellular redox homeostasis [12]. Thus, Cu metabolism and flux have to be strictly controlled for which a multitude of mechanisms exist. Cu is mainly taken up via the high-affinity Cu transporter 1 (Ctr1) [13], and to a lesser extent by Ctr2 [14]. The relevance of the divalent metal-ion transporter 1 (DMT1) for Cu transport is controversially discussed [15,16]. Intracellular Cu is bound to chaperones, which transport Cu to the target proteins [17]. One of these is the Cu chaperone for superoxide dismutase 1 (CCS) [18], which is upregulated when Cu levels are low [19]. Antioxidant protein 1 (Atox1) transfers Cu to ATP7A and ATP7B, essential for Cu export [17]. Further molecules that bind intracellular Cu and thus avoid free ions and/or discharge excessive Cu, are GSH and metallothioneins (MTs) [20–22]. In rodents, Cu deficiency led to a decreased activity of GPXs [23–25]. In addition, Cu is able to reverse selenite-induced cytotoxicity in chicks [26] and in HT29 cells [27]. Based on these studies it is tempting to speculate that Cu interferes with the Se homeostasis. Here we address whether low, adequate or supplemented concentrations of Se and Cu modulate their metabolism *in vitro* and *in vivo*. To this end, we analyzed TE concentrations, gene and protein expression of Se- and Cu-dependent enzymes, and enzyme activities of the selenoproteins GPX and TXNRD in relation to changes in Cu status.

2. Material and methods

2.1. Mouse experiment

Male C57BL/6Jrj mice were housed in polycarbonate cages on a 12:12 h light:dark schedule with constant room temperature (RT, 22 °C) and humidity (55%). After weaning, at the age of 3 weeks, mice received a torula yeast-based Se-deficient diet (modified C1045, Altromin, Lage, Germany) additionally low in Cu and Mn as well as Na (Table 1). For all animals, the deionized drinking water was enriched with Mn and Na, subsequently resulting in 100 ppm and 500 ppm, respectively. Cu and Se were either supplied at suboptimal (no fortification) or adequate (fortification of drinking water, finally 6 ppm and 0.15 ppm, respectively) concentrations. The supply with TEs was weekly adapted to group-specific water and food consumption of the animals to reach the final TE concentration of interest. For supplementation, $CuSO_4$ (Sigma-Aldrich/Merck, Darmstadt, Germany), $MnCl_2$ (Sigma-Aldrich/Merck), NaCl (Sigma-Aldrich/Merck), and Na_2SeO_3 (Thermo Fisher Scientific, Waltham, USA) were employed. The intervention lasted for eight weeks, in which food and water were offered *ad libitum*. Finally, mice were anesthetized with isoflurane (Isothesia, Henry Schein, Hamburg, Germany) and blood was collected by cardiac puncture. Serum was

Table 1
Nutrient requirement of mice [28] and TE content of the diet and drinking water [ppm].

TE	Requirement	Diet	Fortification of drinking water	Final TE supply			
				-Se/-Cu	-Se/+Cu	+Se/-Cu	+Se/+Cu
Cu	6.00	1.60	4.40	1.60	6.00	1.60	6.00
Mn	10.0	8.84	91.2	100	100	100	100
Se	0.15	0.02	0.13	0.02	0.02	0.15	0.15
Na	500	194	306	500	500	500	500

obtained after full coagulation at RT and centrifugation for 10 min (3000×*g*, 4 °C). Organs were surgically dissected and immediately frozen. All animal procedures were approved and conducted following national guidelines of the Ministry of Environment, Health and Consumer Protection of the federal state of Brandenburg, Germany (permission number 2347-44-2017) and institutional guidelines of the German Institute of Human Nutrition Potsdam-Rehbruecke.

2.2. Cell culture

The human hepatocellular carcinoma cell line HepG2 (ACC 180 German Collection of Microorganisms and Cell Cultures (DSMZ)) and the human colorectal adenocarcinoma cell line HT-29 (ACC 299 DSMZ) were cultured in Roswell Park Memorial Institute 1640 media (RPMI; ThermoFisher Scientific) supplemented with 10% (v/v) fetal calf serum (FCS, Sigma-Aldrich/Merck), 1% (v/v) penicillin-streptomycin (P/S; ThermoFisher Scientific), and 1% (v/v) GlutaMAX™ (ThermoFisher Scientific) under standard culture conditions (37 °C, 5% CO_2). Se and Cu are exclusively supplied by the FCS to culture media, resulting in low basal concentrations of 5 nM and 200 nM, respectively. Unless otherwise specified, cells were incubated with 50 nM sodium selenite (99%, Honeywell FlukaTM, Fisher Scientific) or 200 nM selenomethionine (SeMet; Sigma-Aldrich/Merck) and increasing concentrations (25, 50, and 100 μM) of $CuSO_4$ (Sigma-Aldrich/Merck) from the time point of seeding to harvesting 72 h later. When treated with chelators, 400 μM bathocuproinedisulfonic acid (BCS, Sigma-Aldrich) or 75 μM tetrathiomolybdate (TTM, Sigma-Aldrich) were added to the culture medium 24 h before harvesting the cells. For the wash-out experiment, Cu-loaded cells (72 h of incubation) were either left without Cu (-Cu), received Cu super-depletion (-Cu, +BCS), or further Cu treatment (+Cu) for up to 120 h. Cell pellets were frozen in liquid nitrogen and stored at -80 °C until further procedure.

2.3. Cell viability assay

For the MTT assay, cells were seeded in 96-well plates. After 72 h of incubation with Se and Cu, 20 μl of 5 mg/ml thiazolyl blue tetrazolium bromide (MTT; Sigma-Aldrich) was added to the media. After 3 h, media were discarded followed by a 10 min shaking step with 5% (v/v) formic acid (Carl Roth, Karlsruhe, Germany) in 100% isopropanol (Carl Roth) to dissolve the obtained formazan crystals. Absorption was measured at 550 nm with 690 nm as reference wavelength, using a microplate reader (Synergy H1, Biotek, Bad Friedrichshall, Germany). As an additional assay for cell viability, the cell number was determined using a hemocytometer (Neubauer chamber) and trypan blue (Sigma-Aldrich).

2.4. HEK293 reporter gene assay

Three stably transfected human embryonic kidney HEK293 cell lines with either GPX4-specific SECIS element, SECIS-free (negative control) or 100% read-through (positive control) reporter constructs [5] were cultured in Dulbecco's Modified Eagle Medium with high glucose (DMEM; Pan-biotech, Aidenbach, Germany) with 10% (v/v) FCS, 1% (v/v) P/S, and 1% (v/v) Glutamax at 37 °C and 5% CO_2. For reporter gene assay, 20,000 cells per well were seeded in 96-well plates, precoated with poly-L-lysine (Biochrom/Sigma-Aldrich). Cells were incubated with 0, 5, or 10 nM selenite combined with either 0, 1, or 10 μM $CuSO_4$ in DMEM, containing 2.5% (v/v) FCS. As positive control, 50 μg/mL G418 was added in combination with 5 nM selenite. After 72 h of incubation, media were aspirated and 40 μL of 1x lysis buffer (Promocell, Heidenberg, Germany) were added to the wells. After a 10 min shaking step, the plates were put into a freezer to support cell lysis. Renilla luciferase activity was measured after adding 100 μL Coelenterazine (2.5 μg/mL; Promocell) to 35 μL of the cell lysates using luminescence measurement in a microplate reader (Synergy H1). Relative light units (RLU) were normalized to samples incubated with 5 nM Se only for each replicate to obtain relative read-through efficiency.

2.5. RNA isolation, reverse transcription, and quantitative real-time PCR

RNA of snap-frozen liver samples was isolated as previously described [29]. Briefly, total tissue RNA was isolated using Trizol Reagent (Invitrogen, ThermoFisher Scientific). Genomic DNA was eliminated with PerfeCTa DNase I (Quanta BioSciences, Beverly, MA, USA) and reverse transcription was performed using the qScript cDNA synthesis kit (Quanta BioSciences). The mRNA of HepG2 cells was isolated with the Dynabeads mRNA DIRECT kit (ThermoFisher Scientific) according to the manufacturer's description. The mRNA was reversely transcribed using the sensifast™ cDNA synthesis kit (Bioline Meridian Bioscience, Cincinnati, Ohio, USA). Real-time PCRs were performed with 1x PerfeCTa SYBR Green Supermix (Quanta, BioSciences) using cDNA-specific primers (Table 2, Eurofins Genomics, Ebersberg, Germany) at a concentration of 250 nM in a total volume of 10 μL. The Mx3005P QPCR System (Agilent Technologies, Santa Clara, CA, USA) was used with the following heating steps: 3 min at 95 °C, 40 cycles of 15 s at 95 °C, 20 s at 60 °C, and 30 s at 72 °C with all samples and standards measured in triplicates. Standard curves from diluted PCR products were used for quantification. Sample values were normalized to a composite factor based on the reference genes Hprt and Rpl13a. The quantification procedure was performed in accordance with the MIQE guidelines.

2.6. Western blot

To prepare protein lysates, frozen cell pellets or murine tissues were homogenized in Tris buffer (100 mM Tris (Carl Roth), 300 mM KCl (Applichem, Darmstadt, Germany), pH 7.6 with 0.1% (v/v) Triton X-100 (Serva, Heidelberg, Germany), and 0.1% (v/v) protease inhibitor (Merck/Millipore, Burlington, MA, USA)) using a TissueLyser II (Qiagen, Hilden, Germany) by a 2 × 30 s homogenizing step at maximum speed. Cellular debris was removed by centrifugation (14,000 g, 10 min, 4 °C). Protein concentration was determined by Bradford analysis (Bio-Rad Laboratories, Munich, Germany). SDS polyacrylamide gel electrophoresis was followed by immunoblotting of proteins to nitrocellulose membrane. After immunoblotting membranes were gently shaken for 2 min in Ponceau-S solution (0.2% (w/v) Ponceau S (Carl Roth) with 3% (w/v) trichloroacetic acid (Carl Roth) and bands were recorded by ChemiDoc™ MP Imaging System (Bio-Rad). Subsequently, membranes were blocked in 5% (w/v) non-fat dry milk in Tris-buffered saline containing 0.1% (v/v) Tween 20 (T-TBS) for 1 h at RT. The membranes were incubated with the following primary antibodies overnight at 4 °C: rabbit *anti*-GPX1 (3120–1, epitomics, Burlingham, CA, USA, 1:5000), rabbit *anti*-GPX2 ([30], 1:5000), rabbit *anti*-GPX4 (125,066, abcam, Cambridge, UK, 1:5000), rabbit *anti*-TXNRD1 (124,954, abcam, 1:5000), rabbit *anti*-TXNRD2 (180,493, abcam, 1:1000), rabbit *anti*-SELENOH (151,023, abcam, 1:500 (mouse tissue), 1:1000 (cell culture)), rabbit *anti*-MT (192,385, abcam, 1:1000), rabbit *anti*-CCS (137, 131, abcam, 1:5000), rabbit *anti*-NQO1 (34,173, abcam, 1:4000), and rabbit *anti*-SELENOW (600-401-A29, Rockland, Gilbertsville, PA, USA, 1:1000). As secondary antibody horseradish peroxidase-conjugated goat anti-rabbit IgG (1:50,000, 7074S, Cell Signaling, Danvers, MA, USA) was incubated for 1 h in 5% (w/v) non-fat dry milk in T-TBS at RT. Proteins were detected using SuperSignal™ West Dura (ThermoFisher Scientific) and band intensities were quantified densitometrically by the ChemiDoc™ MP Imaging System (Bio-Rad). Protein expression was normalized to ponceau staining.

2.7. Enzyme activities

The protein lysates (see section 'Western blot') were used to measure total activity of GPX [31], TXNRD [32], and NAD(P)H quinone dehydrogenase 1 (NQO1) [33] as described previously. Briefly, GPX activity

Table 2
Primer sequences (5‘ → 3‘).

	Gene	RefSeq-ID	Sequence
mouse	Ccs, Cu chaperone for superoxide dismutase	NM_016892.3	GATGTGATTGGCCGCAGCCT
			CACAGGCCAACCTCTTCCCA
	Hprt, hypoxanthine phosphoribosyltransferase 1	NM_013556.2	GCAGTCCCAGCGTCGTG
			GGCCTCCCATCTCCTTCAT
	Rpl13a, ribosomal protein L13a	NM_009438.5	GTTCGGCTGAAGCCTACCAG
			TTCCGTAACCTCAAGATCTGCT
	Mt1, metallothionein 1	NM_013602.3	CTCCTGCAAGAAGAGCTGCTGC
			CGCTGTTCGTCACATCAGGC
	Mt2, metallothionein 2	NM_008630.2	CTGTGCCTCCGATGGATCCT
			CTTGTCGGAAGCCTCTTTGCAG
human	EEFSEC, selenocysteine-specific elongation factor	NM_021937.3	CCCTAGAGAACACCAAGTTCCGAG
			TCAATGAGCTCTGGAATGCCCT
	GCLM, glutamate-cysteine ligase modifier subunit	NM_002061.3	GTTGACATGGCCTGTTCAGTCCT
			CCCAGTAAGGCTGTAAATGCTCCA
	GPX1, glutathione peroxidase 1	NM_000581.2	TACTTATCGAGAATGTGGCGTCCC
			TTGGCGTTCTCCTGATGCCC
	GPX2, glutathione peroxidase 2	NM_002083.4	GTGCTGATTGAGAATGTGGC
			AGGATGCTCGTTCTGCCCA
	GPX4, glutathione peroxidase 4	NM_002085.3	AGGCAAGACCGAAGTAAACTACAC
			TCTCTTCGTTACTCCCTGGCT
	HPRT, hypoxanthine phosphoribosyltransferase 1	NM_000194.2	TGGCGTCGTGATTAGTGATG
			GGCCTCCCATCTCCTTCAT
	MT2a, metallothionein 2a	NM_005953.3	AGGGCTGCATCTGCAAAGGG
			TAGCAAACGGTCACGGTCAGGG
	NQO1, NAD(P)H quinone dehydrogenase 1	NM_001025434.1	CATCACAGGTAAACTGAAGGACCC
			CTCTGGAATATCACAAGGTCTGCG
	PSTK, phosphoseryl-tRNA kinase	NM_153,336	TTTGAGGCCCAGTCTTGCTACC
			GCCCAACGAATATTTCCGAGCC
	RPL13A, ribosomal protein L13a	NM_012423.2	AGCCTACAAGAAAGTTTGCCTATCTG
			TAGTGGATCTTGGCTTTCTCTTTCCT
	SELENOH, selenoprotein H	NM_170746.2	GCTTCCAGTAAAGGTGAACCCGA
			TCAGGGAATTTGAGTTTGCGTGG
	SELENOP, selenoprotein P	NM_005410	GAAACTCCATCGCCTCATTACCAT
			CTGCCTATGCTGACCCTTGTG
	SELENOW, selenoprotein W	NM_003009.2	GCGGAAGTTGCAGCTACAAGTC
			CGGCTACCATCACTTCAAAGAACC
	SEPHS2, selenophosphate synthetase 2	NM_012,248	GACGGTTTGGGCTTCTTCAAGG
			TCCACAATGCCAACGATCCAC
	SEPSECS,	NM_016955.3	CTAGTGCTCCCGCTTATTCGCC
	Sep (O-phosphoserine) tRNA-Sec tRNA synthase		CTGGACACTTGCCCTTCTCCAG
	TXNRD1, thioredoxin reductase 1	NM_015762.1	GTGTTGTGGGCTTTCACGTACTG
			TGTTGTGAATACCTCTGCACAGAC

was measured using a NADPH-consuming glutathione reductase (GR)-coupled assay, and TXNRD activity was determined by NADPH-dependent reduction of 5,5′-dithio-bis-(2-nitrobenzoic acid) (DTNB) to 2-nitro-5-thiobenzoic acid (TNB). NQO1 activity was conducted using the menadione-mediated reduction of MTT. For measurement of direct effects on the GPX and TXNRD assay both containing EDTA in the reaction mix, Cu, BCS, and TTM were added in increasing concentrations 15 min prior to measuring of enzyme activities to the cell lysates obtained from cells cultured with 50 nM selenite for 72 h. All enzymatic activity measurements were conducted in triplicates using a 96-well plate and a microplate reader (Synergy H1) and were normalized to protein content (Bradford analysis, see section ‘Western blot’).

2.8. Determination of free thiols and total GSH

Measurement of free thiols and GSH was conducted as described earlier [34]. Briefly, supernatants of cultured cells were used to determine free thiols by thiol-mediated reduction of DTNB to TNB. TNB was measured photometrically at 412 nm and normalized to the protein content of the obtained cell lysates. For total GSH determination, cell pellets were lysed in 10 mM HCl (Carl Roth) using ultrasonification (10x, 80% amplitude, 0.5 s) followed by centrifugation (8000×*g*, 30 s, RT) to remove cellular debris. Supernatants were incubated for 10 min with 5% (w/v) 5-sulfosalicylic acid (Sigma-Aldrich) at RT to precipitate proteins. After an additional centrifugation step (8000×*g*, 15 min, 4 °C), samples were used to measure total GSH. The GR-mediated NADPH-consuming reduction of GSSG was coupled to the formation of TNB, which was measured photometrically at 412 nm. The total GSH content was calculated using a standard curve and was normalized to the protein content of samples. For GSH depletion, cells were treated for 24 h with 0.25 mM buthionine-sulfoximine (BSO, Sigma-Aldrich).

2.9. Measurement of Se and Cu content

Cu content of cell lysates and media samples was measured using a bench-top total reflection X-ray fluorescence (TXRF) spectrometer (S2 Picofox™, Bruker Nano GmbH, Berlin, Germany). As internal standard 1 mg/mL Yttrium (Merck/Millipore) was used. 10 µL of each sample were placed on siliconized quartz glass carriers and dried at 40 °C. Samples were measured in duplicates for up to 500 s. Cu and Se content in liver and colon tissue and Se content of HepG2 cells were determined using ICP-MS/MS. Preparation of samples was described previously [29]. Briefly, samples were weighted into PTFE microwave vessels. HNO_3 (65% (v/v), Suprapure®, Merck/Millipore), H_2O_2 (30% (v/v), Sigma-Aldrich/Merck), rhodium (Rh) as internal standard, and ^{77}Se as isotope dilution standard were added before digestion using a Mars 6 microwave digestion system (CEM, Kamp-Lintfort, Germany). After digestion, samples were diluted to achieve final concentrations of 2.93% (v/v) HNO_3, 10 µg/L ^{77}Se, and 1 µg/L Rh. The samples were measured using ICP-MS/MS (8800 ICP-QQQ-MS, Agilent Technologies) and analyzed as described earlier [29]. Certified reference materials, namely fish muscle (ERM BB-422) and pig kidney (ERM BB-186) were used as

quality control of digestion and to cross validate TE analysis using TXRF and ICP-MS/MS.

2.10. Statistics

Data are given as mean + SD. Statistical significance was calculated using GraphPad Prism version 8 (San Diego, CA, USA) with one-way or two-way analysis of variance (ANOVA) and Bonferroni's post-test as indicated in the figure legends. Correlation analysis was performed using calculation of Pearson correlations coefficients. A p-value below 0.05 was considered statistically significant.

3. Results

3.1. Cu inhibits the mRNA expression of GPX1 and selenoprotein W but does not modulate the cellular redox homeostasis

We used data provided via GEO profiles from a microarray study performed in HepG2 cells treated with 100 μM $CuSO_4$ [35]. Searching for selenoprotein transcripts within the whole transcriptome, data revealed that out of the 25 human genes encoding for selenoproteins, seven were detected by this microarray approach. While GPX3 and GPX4 were not significantly modulated by Cu treatment, five transcripts were significantly altered. Out of those, GPX2 and TXNRD1 mRNA levels were upregulated and GPX1, SELENOP, and SELENOW mRNA levels were downregulated. As expected, high fold changes were observed for the two Cu-responsive genes metallothionein MT1A and MT2A (Fig. 1A).

As selenoprotein mRNA levels are also affected by Se, we extended the microarray experiment by adding lower concentrations of $CuSO_4$ (25, 50, and 100 μM) combined with a low or adequate Se supply (0 and 50 nM selenite). Cell number and metabolic activity (MTT reduction activity) as measures for cell viability were unaffected by the two lower doses of $CuSO_4$ while treatment with 100 μM $CuSO_4$ resulted in a reduction of about 20% for both parameters independent of the Se status of the cells (Figs. S1A and B). Using qPCR, we observed a concentration-dependent upregulation of MT2a mRNA by $CuSO_4$ up to a fold change of 20 which was decreased by co-treatment with selenite (Fig. 1B). mRNA levels of GPX1 (Fig. 1C) and SELENOW (Fig. 1D) were significantly downregulated by Cu, but this reduction was only detectable either under -Se conditions for GPX1 or under +Se conditions for SELENOW. In addition, mRNA expression levels of SELENOP (Fig. S1C) and SELENOH (Fig. S1D) showed a trend for a Cu-induced downregulation under -Se conditions. GPX2 mRNA levels were upregulated by Cu (Fig. S1E) while TXNRD1 (Fig. S1F) and GPX4 (Fig. S1G) mRNA levels were unaffected by Cu.

As GPX2 and TXNRD1 are regulated by Nrf2, we next aimed to characterize effects of the experimental set-up on the cellular redox homeostasis. Based on the microarray data, additional Nrf2 target genes were upregulated by Cu including both subunits of the glutamate-cysteine ligase (GCL; Fig. S1H), which could be confirmed by qPCR for GCLM (Fig. S1I). In addition, the Nrf2 target gene NQO1 was significantly induced in the microarray and qPCR (Fig. S1J). However, this effect could not be observed for NQO1 protein expression (Fig. S1K). The intracellular GSH concentration was not affected by Cu but slightly decreased in selenite-treated cells (Fig. S1L), while the concentration of extracellular free thiols was downregulated by Cu independent of the Se supply (Fig. 1M). This indicates that moderately increasing the Cu supply above normal levels does not result in oxidative stress but induces a very mild Nrf2 response.

3.2. Cu modulates protein expression of glutathione peroxidases

Next, we aimed to analyze if the combined Se and Cu treatments not only affect mRNA expression but also protein levels. As expected, protein expression of GPX1, GPX2, GPX4, and SELENOH (Fig. 2A–D) increased in a Se-dependent manner while TXNRD1 and TXNRD2 (Fig. 2E and F) were unaffected by the Se status. The most pronounced inhibitory Cu effects were observed for GPX4 which was decreased by Cu treatment under -Se conditions but rather unaffected under +Se conditions (Fig. 2C). A comparable effect was observed for GPX1 which however only showed a trend for a decreased expression in the 100 μM

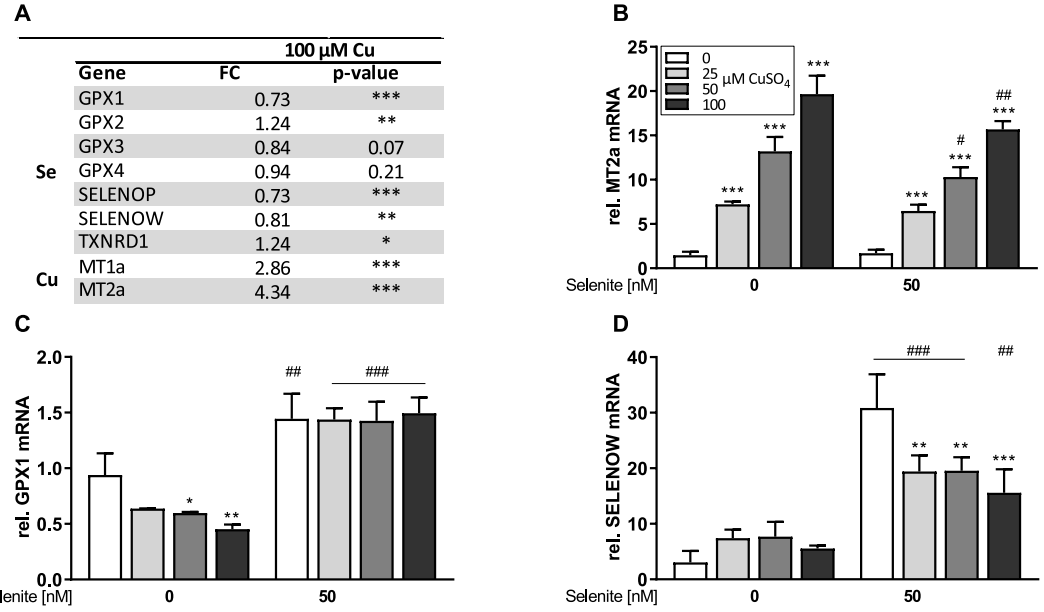

Fig. 1. Expression of Se- and Cu-dependent genes in HepG2 cells. Microarray data provided by GEO Profiles (GEO Series Accession No. GSE9539) [35] obtained from HepG2 cells treated for 24 h with 100 μM $CuSO_4$ (A). Data are given as fold change (FC) relative to the untreated control (n = 3). qPCR results of various Se- and Cu-responsive genes analyzed in HepG2 cells cultured with increasing Cu concentrations (0, 25, 50 or 100 μM) combined with or without 50 nM selenite for 48 h (B–D). Gene expression was normalized to the reference genes RPL13A and HPRT. Untreated cells of the first replicate were set as 1. Data are depicted as mean + SD (n = 3). Statistical analyses were based on two-way ANOVA with Bonferroni's post-test. *p < 0.05; **p < 0.01; ***p < 0.001 vs. 0 μM $CuSO_4$ and $^{\#}$p < 0.05; $^{\#\#}$p < 0.01; $^{\#\#\#}$p < 0.001 vs. 0 nM Se.

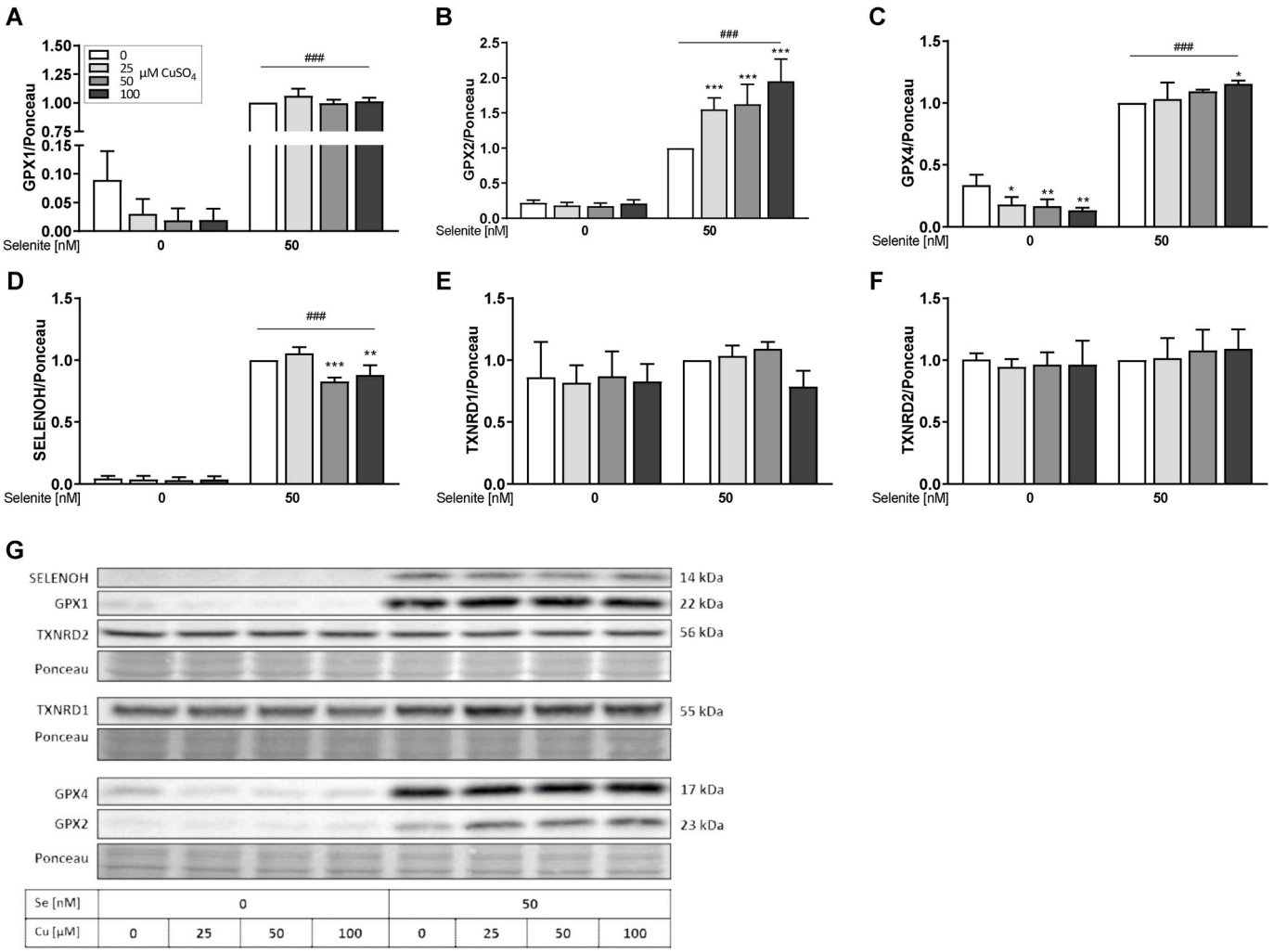

Fig. 2. Cu modulates the expression of several selenoproteins. HepG2 cells were treated with increasing Cu concentrations (0, 25, 50 or 100 µM) in combination with or without 50 nM selenite for 72 h. Protein expression was determined using Western blot, normalized to Ponceau staining. Samples with Se treatment and without Cu were set as 1 (A–F). Representative blots are shown (G). Data are depicted as mean + SD (n = 3-4). Statistical analyses were based on two-way ANOVA with Bonferroni's post-test. *$p < 0.05$; **$p < 0.01$; ***$p < 0.001$ vs. 0 µM $CuSO_4$ and $^{###}p < 0.001$ vs. 0 nM Se.

Cu treatment group without Se ($p = 0.08$) (Fig. 2A). In contrast, GPX2 protein expression was unaffected by Cu under -Se conditions but increased with Cu treatment under +Se conditions (Fig. 2B). SELENOH, TXNRD1, and TXNRD2 (Fig. 2D–F) protein expression levels were rather unaffected by Cu treatment. The expression of the Cu marker proteins MT and CCS was not modulated by any of the treatment conditions (Figs. S2A–C).

3.3. GPX and TXNRD activities are downregulated by Cu treatment

Next, we aimed to identify potential Cu effects on total enzyme activities of GPX and TXNRD. Both GPX and TXNRD activities were upregulated by an increasing Se supply (Fig. 3A, C). Cu treatment resulted in a significant decrease of total GPX activity down to about 80% which was, however, only detectable in selenite-treated cells (Fig. 3A). In contrast, TXNRD activity was inhibited by Cu to about 50% which was independent of the cellular Se status (Fig. 3C). These Cu-induced effects on GPX and TXNRD activities were confirmed using another cell line, namely HT-29 (Figs. S3A and B). In addition, we used SeMet as an alternative selenocompound for studying interactions between Cu and Se. Also in SeMet-treated cells, Cu co-treatment efficiently inhibited GPX and TXNRD activities (Figs. S3C and D). To exclude that Cu directly interfered with the assays, e.g. by binding to NADPH, increasing Cu concentrations were added to the reaction mixture of the GPX (Fig. 3B) or TXNRD (Fig. 3D) assay 15 min prior to measurement. None of the tested Cu concentrations affected the GPX assay (Fig. 3B). TXNRD activity was stable up to 1 µM of added Cu but inhibited by a very high $CuSO_4$ concentration of 100 µM (Fig. 3D). But even this high Cu concentration was not resulting in a comparable inhibition of TXNRD activity as observed in cultured cells (Fig. 3C).

3.4. Cu treatment decreases read-through and thus UGA recoding efficiency

To clarify whether Cu affects the selenoprotein synthesis machinery, mRNA expression levels of genes encoding for factors essential for selenoprotein synthesis were analyzed. Out of the four tested genes, only SEPHS2 was sensitive towards the Se status and was downregulated under conditions of Se supply (Fig. 4A). SEPSECS expression was diminished upon treatment with 100 µM $CuSO_4$ which was only observed under +Se conditions (Fig. 4B). PSTK and EEFSEC expression was neither affected by Se nor by Cu treatment (Figs. S4A and B). To verify intracellular Se availability for cells upon Cu treatment, the cellular Se content was determined. The Se content was increased with increasing Cu concentrations and was almost doubled with highest Cu concentration under +Se conditions. Under -Se conditions, there was no

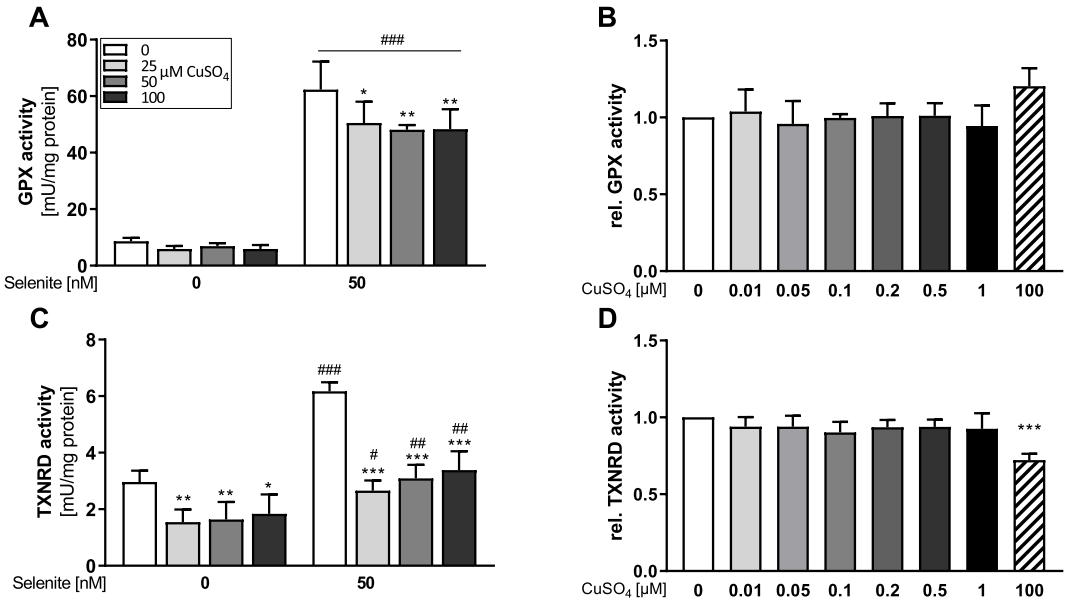

Fig. 3. Cu decreases selenoprotein activity, but does not directly affect enzyme activity within the assay. HepG2 cells were cultured with increasing Cu concentrations (0, 25, 50 or 100 µM) in combination with or without 50 nM selenite for 72 h (A, C). Lysates of selenite supplemented (50 nM for 72 h) cells were used to measure the direct impact of Cu on enzyme activities (B, D). Increasing concentrations of Cu were added 15 min prior to measurement of enzyme activities and were normalized to lysates without additional Cu. Activities of GPX (A, B) and TXNRD (C, D) were measured photometrically and normalized to protein content. Data are depicted as mean + SD (n = 3-4). Statistical analyses were based on two-way ANOVA with Bonferroni's post-test (A, C) or one-way ANOVA (B, D) with Bonferroni's post-test. *$p < 0.05$; **$p < 0.01$; ***$p < 0.001$ vs. 0 nM $CuSO_4$ and $^{\#}p < 0.05$; $^{\#\#}p < 0.01$; $^{\#\#\#}p < 0.001$ vs. 0 nM Se.

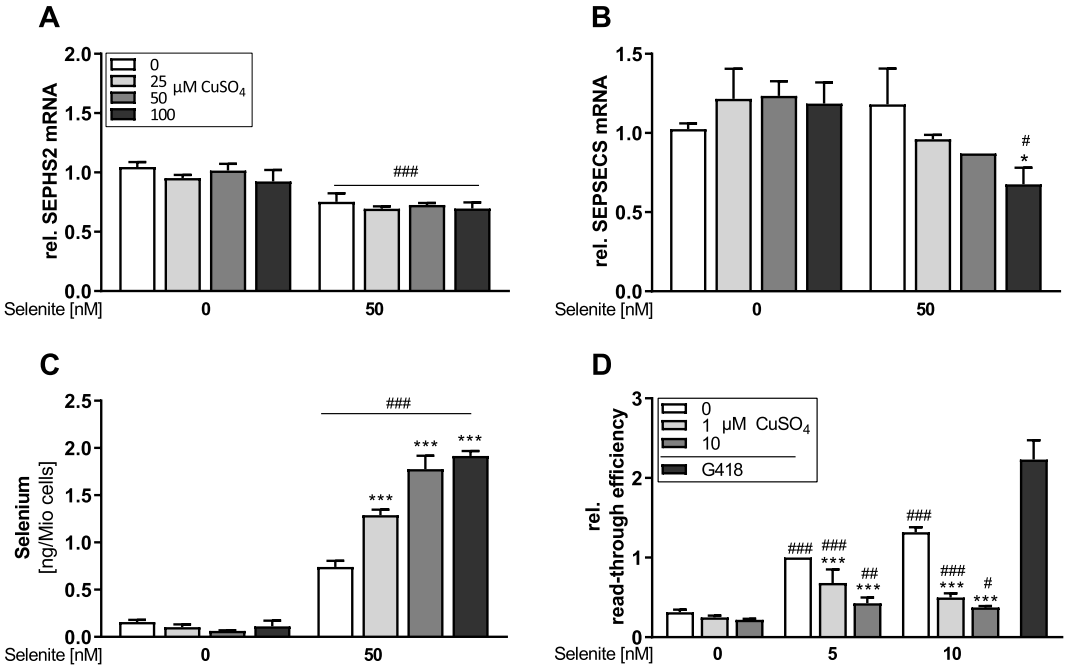

Fig. 4. Cu affects gene expression of the selenoprotein synthesis machinery, the cellular Se content and read-through efficiency. HepG2 cells were cultured with increasing Cu concentrations (0, 25, 50 or 100 µM) in combination with or without 50 nM selenite for 48 h. Gene expression was analyzed by qPCR and normalized to the reference genes RPL13A and HPRT (A, B) and untreated cells of first replicate were set as 1. The Se content of cell lysates was measured using ICP-MS/MS (C). Read-through efficiency was measured using HEK293 cells stably transfected with a reporter gene vector containing the SECIS element of GPX4. Cells were cultured with 1 or 10 µM $CuSO_4$ in combination without or with 5 and 10 nM selenite for 72 h. Read-through efficiency was determined by luminescence measurement and was shown relative to cells treated with 5 nM selenite (D). G418 (+5 nM Se) was used as positive control. Data are depicted as mean + SD (n = 3). Statistical analyses were based on two-way ANOVA with Bonferroni's post-test. *$p < 0.05$; ***$p < 0.001$ vs. 0 µM $CuSO_4$ and $^{\#}p < 0.05$; $^{\#\#}p < 0.01$; $^{\#\#\#}p < 0.001$ vs. 0 nM Se.

Cu effect on intracellular Se levels (Fig. 4C). Another way of modulating selenoprotein expression is via affecting the SECIS read-through efficiency. We used the SECIS element of GPX4 to test for a potential Cu effect. Cu downregulated the read-through efficiency in a concentration-dependent manner under +Se conditions. G418 was used as a positive control and doubled read-through efficiency (Fig. 4F). Both, control cells

transfected with the positive control vector with 100% read-through and the SECIS-free negative control vector were unaffected by Cu treatment (Figs. S4C and D).

3.5. Reversal of Cu effects on selenoprotein expression and activity by Cu chelators

To study the Cu specificity of the effects observed, we established treatment conditions with two different Cu specific chelators, namely BCS and TTM. The Cu content of the cells increased by Cu treatment but remained unaffected by Se co-treatment (Fig. 5A). After 24 h of BCS treatment, the intracellular Cu content decreased to 55%, whereas intracellular Cu increased in response to TTM treatment (Fig. 5A). These findings are supported by previously published data showing that BCS is an extracellular chelator [36]. BCS efficiently decreased the intracellular Cu content not only after 24 h of treatment (Fig. 5A), but also over a period of five days, when supplied to Cu-supplemented cells (Fig. S5A). BCS was able to sequester Cu from cells which resulted in Cu accumulation in the media (Fig. S5B). In contrast, TTM is known to be taken up into cells and is supposed to bind and accumulate Cu there [36] which results in higher cellular Cu levels (Fig. 5A). However, this TTM-bound Cu is not available as free Cu and is thus less bioactive.

Accordingly, co-treatments with each of the two chelators were used to test whether Cu-induced effects on selenoproteins and Cu-related biomarkers can be reversed. The Cu-induced increase of MT2a mRNA expression was efficiently diminished by the two chelators, but most strongly by BCS reaching almost basal MT2a expression levels (Fig. 5B). Again, MT2a expression was also repressed by an increasing Se supply. CCS protein expression was increased when TTM but not BCS was added to the -Cu groups (Fig. 5C). The Cu-induced downregulation of SEPSECS was reversed by BCS, but not by TTM (Fig. 5D). Co-treatment with each of the two chelators blocked the Cu-induced inhibition of GPX activity (Fig. 5E). The protein expression of different GPXs again was only marginally affected (Figs. S5C and D). We also measured a putative direct influence of BCS and TTM on the GPX activity assay, which was not observed (Figs. S5G and H). The Cu-induced inhibition of TXNRD activity was not only reversed by BCS treatment, but TXNRD activity even further increased above basal levels. In contrast, TTM did not reverse the Cu-mediated inhibition of TXNRD activity. Interestingly, TXNRD activity was generally increased in TTM-treated cells (Fig. 5F). Although effects on TXNRD activity were detectable, the protein expression of neither TXNRD1 nor TXNRD2 was affected by Cu or the chelators (Figs. S5E and F). As shown for GPX activity, the two chelators had no direct effect on the TXNRD activity assay (Figs. S5I and J).

3.6. In vivo interactions of Se and Cu

To further elucidate if Cu interferes with selenoprotein synthesis and activity also *in vivo*, we performed a mouse study with suboptimal or adequate amounts of Se and Cu supplied by the drinking water. The Se and Cu status of all mice was characterized by measuring the concentrations of both TEs in liver samples as the central metabolic organ for TEs and in colon samples to study local effects between the luminal content and the organism. The Se concentrations of both liver (Fig. 6A)

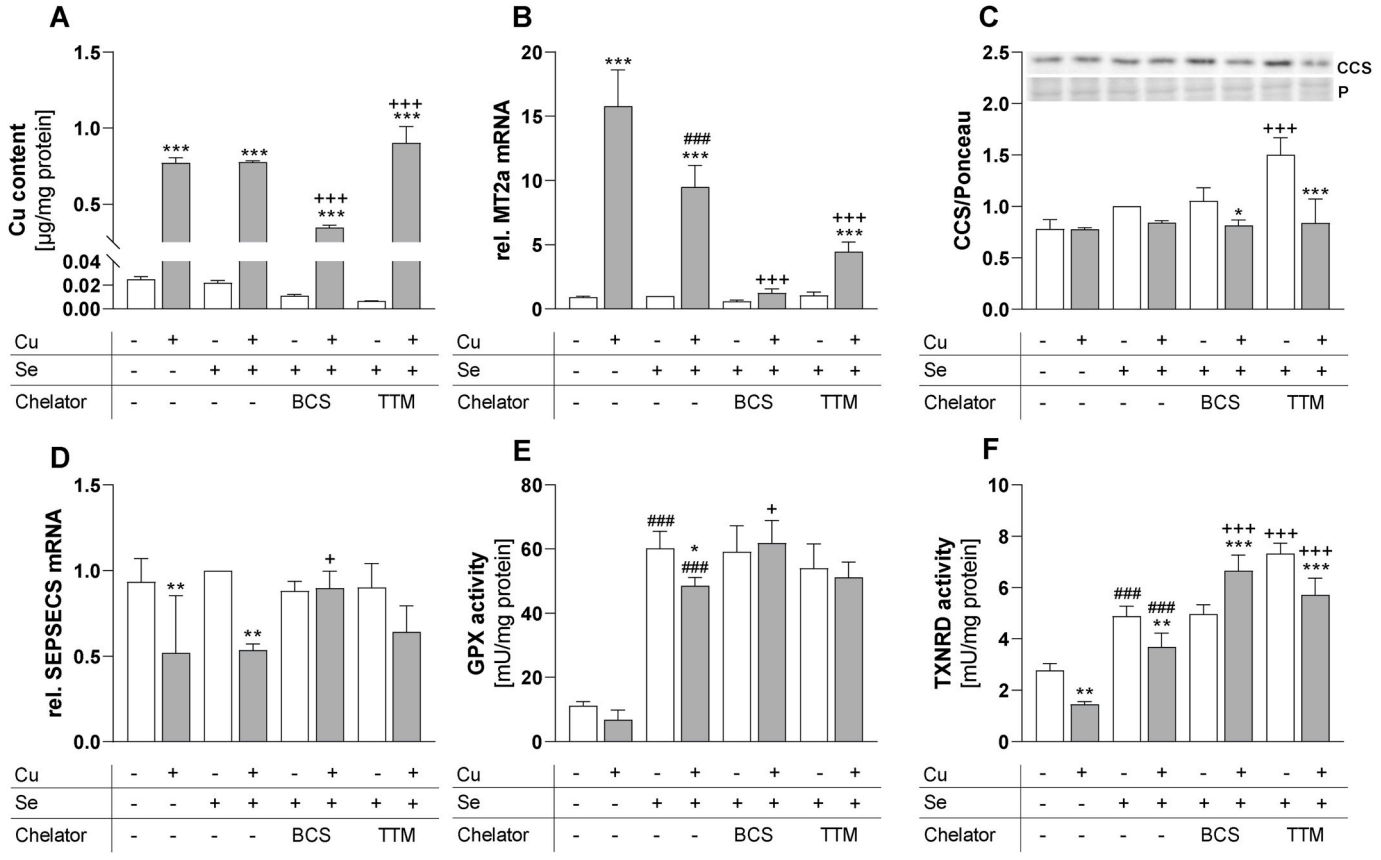

Fig. 5. Cu-induced effects could be reversed by co-treatment with the Cu chelators BCS and TTM. HepG2 cells were treated with 100 µM $CuSO_4$ in combination with or without 50 nM selenite for 72 h. After 48 h of incubation, the two chelators bathocuproine disulfonic acid (BCS, 400 µM) or tetrathiomolybdate (TTM, 75 µM) were added to the cells. Cu content (A) was measured using TXRF and normalized to protein content. Gene expression (B, D) was determined via qPCR and normalized to the reference genes RPL13A and HPRT. Protein expression (C) was normalized to Ponceau staining (P). Cells with Se, but without chelator or Cu treatment were set as 1. Enzyme activities of GPX and TXNRD (E, F) were measured photometrically. Data are depicted as mean + SD (n = 4). Statistical analyses were based on two-way ANOVA with Bonferroni's post-test. *$p < 0.05$; **$p < 0.01$; ***$p < 0.001$ vs. 0 µM $CuSO_4$; $^{###}p < 0.001$ vs. 0 nM Se, and $^{+}p < 0.05$; $^{+++}p < 0.001$ vs. -chelator.

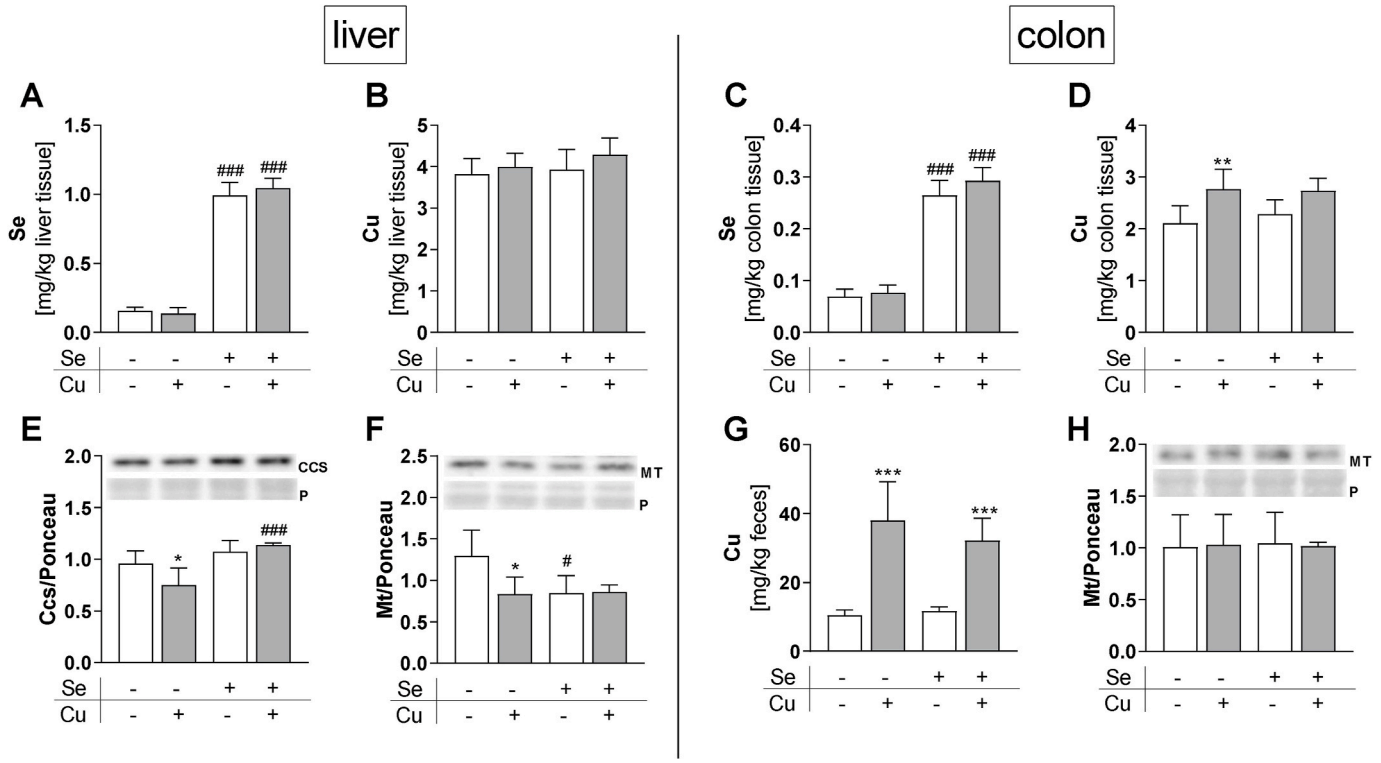

Fig. 6. Dietary intervention with the TEs Cu and Se. Se and Cu contents in liver (A, B), and colon (C, D) of mice supplied with suboptimal (0.02/1.6 ppm) or adequate (0.15/6 ppm) amounts of Se and Cu were determined using ICP-MS/MS. Protein expression (E, F, H) was normalized to Ponceau staining (P). Data are depicted as mean + SD (n = 5). *p < 0.05; ***p < 0.001 vs. -Cu; $^{\#}$p < 0.05; $^{\#\#}$p < 0.01; $^{\#\#\#}$p < 0.001 vs. -Se calculated based on two-way ANOVA with Bonferroni's post-test.

and colon (Fig. 6C) were strongly different in relation to the Se supply, indicating that the feeding conditions were well suitable to modulate the Se status. However, even though there was a 3.75-fold difference in Cu supply between -Cu and +Cu mice, no differences in hepatic Cu levels were observed (Fig. 6B). A difference in Cu concentrations was detectable in the colon only (Fig. 6D), which was even far more pronounced in the feces (Fig. 6G). To further characterize the Cu status of the mice, expression levels of Cu-dependent proteins were analyzed. Hepatic Ccs protein expression was downregulated by Cu which was, however, only detectable under -Se and not under +Se conditions (Fig. 6E). Ccs transcript levels were not significantly modulated by Cu or Se in the liver (Fig. S6A). Mt protein expression was upregulated under conditions of low Se and Cu supply in the liver (Fig. 6F), but not in the colon (Fig. 6H). The mRNA expression in the liver of both, Mt1 and Mt2 was not significantly affected by Se or Cu (Figs. S6B and C) but revealed a comparable pattern as shown on protein level with higher expression under -Cu/-Se conditions. Based on this, we concluded that the Se status was successfully modulated systemically while the Cu status was only locally modulated in the colon and not in the liver.

Next, we studied whether the Cu-induced effects on selenoproteins can be detected *in vivo* despite the marginal changes in systemic Cu status. While hepatic Gpx activity was not modulated by Cu (Fig. 7A), hepatic Txnrd activity was repressed as already observed *in vitro*, however to a smaller extent and only under +Se conditions (Fig. 7B). Hepatic selenoprotein expression was not affected by Cu (Fig. 7E, F, I, J, S6D-F). In the colon, neither Gpx (Fig. 7C) nor Txnrd (Fig. 7D) activity was downregulated by Cu, which was in line with stable Txnrd1 and Txnrd2 protein expression (Fig. 7G and H). In contrast to the *in vitro* results, colonic protein expression of Gpx1 was not downregulated but even upregulated by Cu under +Se conditions (Fig. 7K). Also, Selenoh showed a Cu-induced upregulation of protein expression in colon tissue (Fig. 7L). Hepatic Nqo1 activity was not affected by the Cu supply (Fig. S6K).

4. Discussion

Metabolism of the single TEs, Se and Cu, is characterized well, but interactions of both are rarely investigated. Therefore, we addressed the question of whether Cu interferes with Se metabolism in *in vitro* and *in vivo* experiments. We performed a mouse feeding study with suboptimal (0.02/1.6 ppm) and adequate (0.15/6 ppm) amounts of Se and Cu, respectively, which were supplied via the drinking water. This way, we aimed to address dietary changes of these two TEs in a physiologically relevant concentration range. For Se, both the hepatic concentration (Fig. 6A) and total Gpx activity (Fig. 7A) were downregulated to 14% or 4% in relation to the +Se group, which is in line with previous feeding experiments using the Se-deficient torula yeast diet [37,38]. However, the Cu status was affected only marginally by our intervention, because the low Cu content of the diet was obviously enough to maintain Cu homeostasis efficiently. Hepatic Cu concentrations were unaffected (Fig. 6B) which has previously been described with an even lower Cu supply [39]. Hepatic Cu only responds to severe feeding-induced Cu deficiencies [19,40,41] or in knockout mouse models e.g., for Ctr [42,43] or Atp7b [44]. Even though, there was no effect on Cu concentrations, Cu-responsive proteins such as Mt and Ccs were upregulated in the -Se/-Cu group (Fig. 6E and F). In contrast to the liver, the Cu concentration was decreased by the low Cu diet in the colon (Fig. 6D) but the effect was rather small. In response to low dietary intake, the intestinal Cu absorption strongly increases in mice [39] and in humans [45], leading to very low fecal content compared to adequately Cu-supplied mice [39]. Also herein, the treatment effect on the fecal Cu concentration was most pronounced (Fig. 6G). Overall, we successfully modulated the Se status whereas the Cu status remained largely unaffected by our experimental design.

The following results were obtained regarding *in vivo* interactions of both elements: (1) no effect on Cu levels in colon and liver after modulating the Se status from an adequate towards a suboptimal supply.

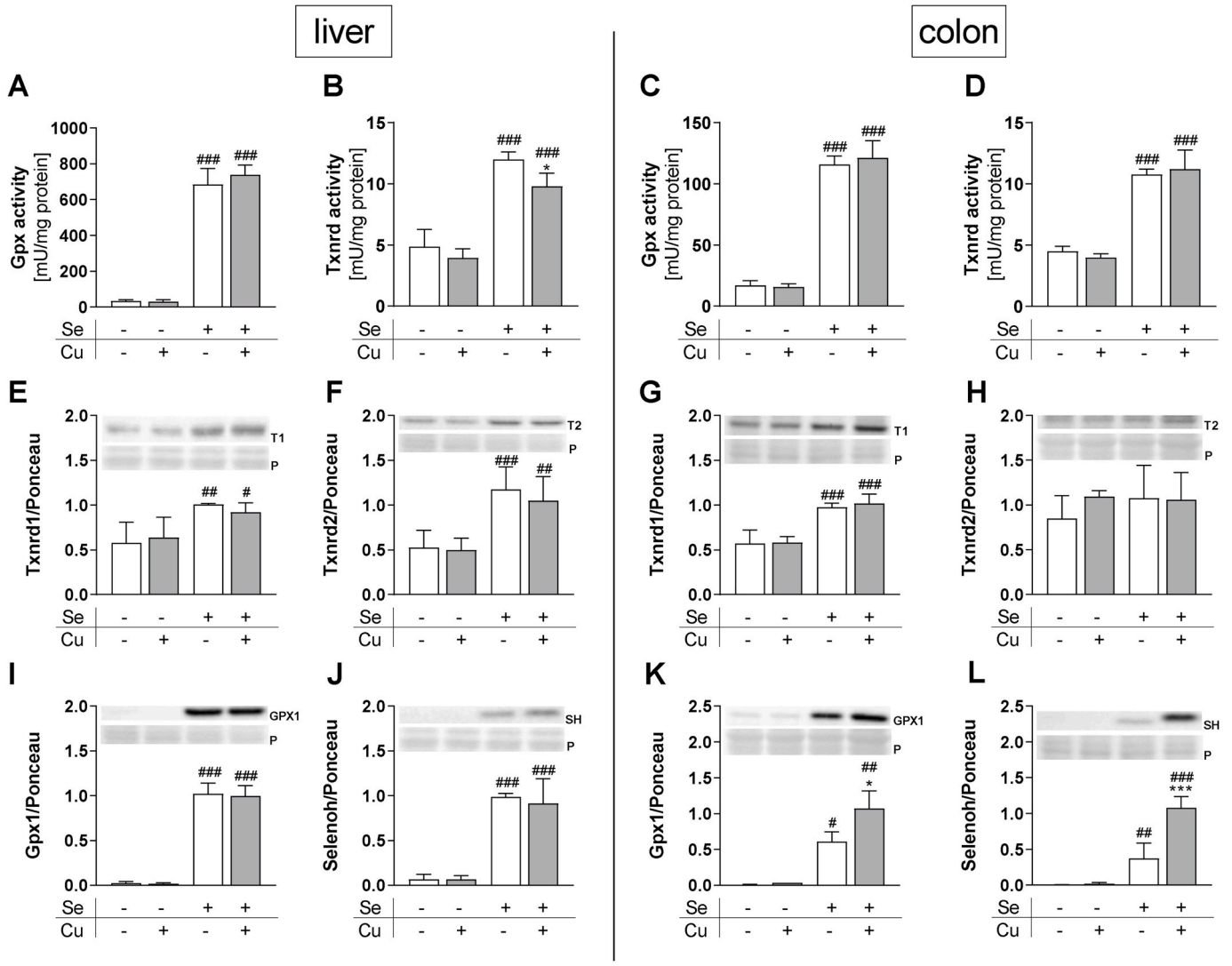

Fig. 7. Activity and expression of selenoproteins in vivo. Enzyme activities of GPX (A, C) and TXNRD (B, D) and selenoprotein expression in liver and colon (E–L) of mice supplied with suboptimal (0.02/1.6 ppm) or adequate (0.15/6 ppm) amounts of Se and Cu were determined photometrically or using Western blot, respectively. Proteins (T1 = Txnrd1; T2 = Txnrd2; SH = Selenoh) were normalized to Ponceau staining (P). Data are depicted as mean + SD (n = 5). $^{*}p < 0.05$; $^{***}p < 0.001$ vs. -Cu; $^{\#}p < 0.05$; $^{\#\#}p < 0.01$; $^{\#\#\#}p < 0.001$ vs. -Se calculated based on two-way ANOVA with Bonferroni's post-test.

This is in line with previous studies showing stable hepatic Cu levels with increasing Se concentrations [46,47]. However, we observed Cu-induced effects on Cu-responsive proteins such as Mt and Ccs (Fig. 6E and F) that were more pronounced under Se deficiency compared to an adequate Se supply indicating an interplay which warrants further investigation. (2) *Vice versa*, we did not observe any effect of Cu on the Se concentration in the liver or colon, but this might be due to the fact that the Cu status was only very marginally affected by our dietary intervention. Unexpectedly, we observed an upregulation of Gpx1 and Selenoh in the colon of the +Se/+Cu group (Fig. 7K and L). Atp7b knockout mice with hepatic Cu accumulation have increased levels of Selenoh in liver nuclei. The nuclear abundance of Selenoh in these mice is supposed to be connected to oxidative stress as a result of excessive Cu accumulation [48]. However, this is unlikely to be the case in our +Se/+Cu mice, as the activity of the Nrf2 target gene Nqo1 as indicator for the hepatic redox balance was not increased but rather decreased in mice of this group (Fig. S6K). In sheep, an increase in hepatic Se concentrations was observed following Cu administration [49] which was also observed herein in HepG2 cells (Fig. 4C).

Thus, under low to adequate conditions, there are only modest interactions of Se and Cu, however, when considering adequate to supplemented Cu concentrations, as we did in our *in vitro* experimental setting, we observed that Cu substantially interferes with selenoprotein synthesis at different levels. First, there was a Cu-dependent downregulation of transcript levels of GPX1, and SELENOW which are known to be sensitive towards a limited Se supply [50,51]. Cu even enhanced the decrease of GPX1 under low Se conditions (Fig. 1C), thus, worsening functional consequences of a Se deficiency. Interestingly, mRNA levels of SELENOW were only downregulated by Cu under conditions of an adequate Se supply (Fig. 1D) indicating that in case of SELENOW obviously higher Se concentrations are needed to upregulate mRNA levels when Cu levels are high. So far, Cu effects have been attributed mainly to an increase in oxidative stress upon Cu treatment. However, this is not likely to be the case in our experimental setting. If the cellular redox homeostasis is of relevance here, one would expect an upregulation of selenoprotein transcripts by Cu instead of a downregulation [9], which we also observed for Nrf2 target genes (Figs. S1E and F, H–K). In previous experiments, incubation of HepG2 or neuroblastoma cells with 200 μM Cu decreased p53 reporter activity and mRNA expression of GPX1 [52,53], which is known to be regulated via p53 [54,55]. However, the inhibition of p53 activity by Cu was observed with 200 μM only and not with lower Cu concentrations [52] which we used herein.

SELENOH and SELENOW have been described as target genes of the metal regulatory transcription factor 1 (MTF-1), but only SELENOH expression is decreased by MTF-1 e.g., in zinc-treated cells [56]. As Cu also enhances transactivation of MTF-1 [57], this could potentially be involved in the regulation of the indicated selenoprotein mRNA levels.

Second, Cu downregulated SEPSECS mRNA expression (Fig. 4B) and read-through efficiency exemplarily shown for the SECIS element of GPX4 (Fig. 4D) indicating that Cu repressed selenoprotein synthesis. SEPSECS expression has been previously shown to be decreased during acute phase response in lipopolysaccharide-treated mice [58]. Interestingly, the effects on SEPSECS and on read-through efficiency were observed in Se-treated cells only. Thus, even though the cells accumulated more Se when co-treated with Cu (Fig. 4C), they use this Se less efficiently to synthesize selenoproteins. This is also in line with the previous finding that selenoprotein mRNAs which are most sensitive towards limited Se availability (such as GPX1) mostly react on the Cu supply. Interestingly, it has been shown that remodeling of the RNA processing machinery is taking place in cells with elevated Cu [48]. Via this mechanism Cu could also interfere with selenoprotein synthesis.

The UGA recoding event is the rate limiting step of selenoprotein expression. Besides Se bioavailability, other exogenous stimuli are discussed to be modulators of Sec insertion efficiency [59]. The Cu status obviously is one of them. However, the Cu effects on read-through efficiency are mirrored only marginally on the protein levels, the third level of interaction between Cu and selenoproteins. For GPX4, a decreased expression following Cu incubation was observed under low Se conditions only, while especially GPX2 was upregulated by Cu under adequate Se conditions (Fig. 2B and C). As shown before, protein levels of selenoproteins are not very informative here because impairments of read-through efficiency could result in enhanced misincorporation of wrong amino acids instead of Sec. This effect has previously been observed after cells were treated with different antibiotics. Especially GPX1, GPX4, and TXNRD1 were highly sensitive towards replacement of Sec by cysteine or aginine [60]. Also under Se deficiency, an alternative aminoacylation of the $tRNA^{Ser/Sec}$ with cysteine has been proposed resulting in cysteine variants of selenoproteins with lower enzymatic activity [61–63]. Indeed, the fourth level of Cu-induced modulation takes place at the activity level, where both total GPX and particularly TXNRD activity are inhibited by Cu. This inhibition was observed in two cell lines (HepG2 and HT29 cells) and upon co-treatment with any of two different selenocompounds, i.e., selenite and SeMet (Fig. 3A, C; S3A-D). In both cases, activity levels cannot be directly explained by changes in protein expression. All three GPXs (GPX1, 2, and 4) are unaffected or even increased by Cu under Se adequate conditions which was also the case for TXNRD1 and TXNRD2 (Fig. 2A–C, E, F). Based on this, we were wondering whether Cu can directly interfere with enzymatic assay conditions, e.g., by binding to NADPH but this was not the case, at least for the Cu concentrations that we presumably reached in our cell lysates (Fig. 3B, D). However, we could show that extracellular thiol concentrations were decreased upon Cu treatment (Fig. S1M) indicating that Cu modulates the cellular redox balance as previously extensively discussed [64]. Interestingly, previous results on the influence of Cu on GPX activity were rather heterogeneous. Similar to the data presented, treatment with 100 μM Cu showed no effect on GPX activity in HepG2 cells when no further Se was added to cells [65]. In contrast to our results, GPX activity has been reported to be decreased in Cu deficient liver and plasma of mice and rats [23–25]. However, in line with our results GPX activity was significantly lower in LEC rats, an animal model for Wilson's disease, with hepatic Cu accumulation in comparison to rats with lower Cu levels [66], and in Wistar rats that received an injection with Cu [67]. A lower activity of the antioxidant enzymes GPXs and TXNRDs by higher levels of Cu could contribute to Cu-induced oxidative damage and thus amplify the severity of liver disease. Also in Wilson's disease patients hepatic GPX activity is inhibited but only at stage III. The authors concluded from this result that GPX expression is first enhanced in early stages and is decreased only when the liver is severely damaged [68]. Regarding this hypothesis, we can exclude cytotoxic Cu effects for the Cu concentrations that we used herein as mechanism for the observed inhibition of GPX activity. In another clinical study on Wilson's disease, treatment naive patients were compared with patients receiving Cu reducing therapy. In those patients, higher serum Cu levels were associated with higher and not lower whole blood GPX activity [69]. For Cu effects on TXNRD activity, little data is available from the literature. But there are many well established metal- and semimetal-containing TXNRD inhibitors [70]. Here, the *in vitro* inhibition of TXNRD activity could be recapitulated in the liver of +Se/+Cu compared to +Se/-Cu mice but not in the colon though the hepatic Cu status was only very marginally affected by our intervention (Fig. 6B; 7B). Thus, Cu effects on selenoprotein activity obviously depend on multiple factors including the Cu concentration range and the organ analyzed.

To mechanistically extent the *in vitro* results, we used the two Cu chelators BCS and TTM [42,71]. Two distinct modes of action may underlie the effects observed for BCS: i) Cu is chelated and retained in the media leading to a 50% reduction of intracellular Cu content (Fig. 5A), and ii) Cu is efficiently drained from inside the cell resulting in a super-depletion indicated by lower intracellular and higher extracellular Cu over time in comparison to cells without further BCS treatment during wash out (Figs. S5A and B). In contrast, TTM treatment results in higher intracellular Cu concentrations than in untreated cells [72,73]. Thus, treatment with both chelators resulted in decreased Cu bioavailability for the cells, but BCS appeared to be more efficient because the enhanced MT2a gene expression with Cu treatment was more strongly diminished with BCS than with TTM (Fig. 5B). This has previously also been shown in human neuroblastoma cells [74]. The observed effects on SEPSECS mRNA expression, GPX4 protein expression and on GPX and TXNRD activity were successfully reversed by chelator treatment and are thus Cu specific (Fig. 5D–F; S5C). In addition, there was a clear dependency of TXNRD activity and to a lesser extent for GPX activity on Cu availability. Cells with the lowest Cu availability (BCS-treated cells in combination with Cu and TTM without Cu) had the highest levels of TXNRD activity resulting in an inverse correlation (Fig. 8A and B). The correlation was stronger for TXNRD activity than for GPX activity.

In summary, Cu concentrations up to 100 μM inhibit activities of GPX and TXNRD *in vitro*. However, *in vivo* the effects were rather small under conditions of a mild modulation of the Cu status in the adequate to suboptimal concentration range in healthy, young mice. The average human serum concentration of Cu ranges from 15 to 31.5 μM [75–77], and thus concentrations used in cell culture experiments are adequate to supplemented. But under pathophysiological conditions up to 200 μM Cu were reported in serum [78]. In liver samples of patients with Wilson's disease or of Indian childhood cirrhosis Cu concentrations of 1.142 mg/g dry weight and 4.788 mg/g dry weight, respectively, were observed [79]. This shows that very high values of Cu can be achieved in certain diseases indicating the high relevance of our *in vitro* results. Under these conditions, not only the increase in Cu levels but a potential concomitant functional decrease of selenoproteins might by driving factors for disease progression. Also under physiological conditions, serum Cu concentrations can be increased as recently described when comparing a subcohort of the EPIC Potsdam cohort which has been reinvited after 20 years. Advanced age was associated with increased Cu concentrations and decreased Se concentrations [76]. This indicates that an age-related decline in selenoprotein expression most probably is a result of a combination of lower Se concentrations and higher Cu concentration. Also during disease, the Se to Cu ratio is frequently altered, most likely as a response to acute or chronic inflammation [80,81]. Accordingly, a higher Se intake would be needed to overcome the Cu-induced suppressive effects. These findings indicate that it is meaningful to study interactions of Se and Cu, and to understand the consequences and underlying mechanisms of this interplay in order to identify measures that may help to achieve and maintain health-supporting concentrations of these redox-relevant TEs.

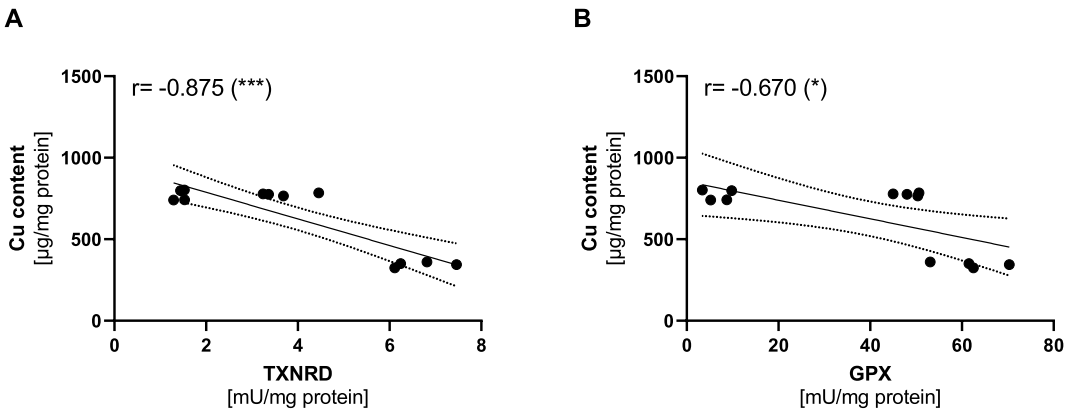

Fig. 8. Correlation of intracellular Cu content with enzyme activities of TXNRD and GPX. Correlation analysis of intracellular Cu content and enzyme activity of TXNRD (A) and GPX (B) was performed using data of HepG2 cells treated with 100 µM $CuSO_4$ with or without 50 nM selenite for 72 h. After 48 h of incubation, the two chelators bathocuproine disulfonic acid (BCS, 400 µM) or tetrathiomolybdate (TTM, 75 µM) were added to the cells. The TTM + Cu group was excluded from analysis because of the accumulation of non-bioactive but quantifiable intracellular Cu. *$p < 0.05$; ***$p < 0.001$ calculated based on Pearson correlation coefficient.

Conflicts of interest

The authors declare that they do not have any conflict of interest.

Funding

This work was supported by the German Research Foundation (DFG), Germany, FOR 2558 (KI 1590/3-2).

Acknowledgement

The authors highly acknowledge the excellent technical support by Stefanie Deubel, Alrun Schumann, and Doreen Ziegenhardt.

Appendix A. Supplementary data

Supplementary data to this article can be found online at https://doi.org/10.1016/j.redox.2020.101746.

References

[1] G.V. Kryukov, et al., Characterization of mammalian selenoproteomes, Science 300 (5624) (2003) 1439–1443.
[2] V.M. Labunskyy, D.L. Hatfield, V.N. Gladyshev, Selenoproteins: molecular pathways and physiological roles, Physiol. Rev. 94 (3) (2014) 739–777.
[3] K.Y. Ko, et al., S-Glutathionylation of mouse selenoprotein W prevents oxidative stress-induced cell death by blocking the formation of an intramolecular disulfide bond, Free Radic. Biol. Med. 141 (2019) 362–371.
[4] K. Renko, et al., Aminoglycoside-driven biosynthesis of selenium-deficient Selenoprotein P, Sci. Rep. 7 (1) (2017) 4391.
[5] J. Martitz, et al., Factors impacting the aminoglycoside-induced UGA stop codon readthrough in selenoprotein translation, J. Trace Elem. Med. Biol. 37 (2016) 104–110.
[6] D.E. Handy, et al., Aminoglycosides decrease glutathione peroxidase-1 activity by interfering with selenocysteine incorporation, J. Biol. Chem. 281 (6) (2006) 3382–3388.
[7] A. Banning, et al., The GI-GPx gene is a target for Nrf2, Mol. Cell Biol. 25 (12) (2005) 4914–4923.
[8] A. Sakurai, et al., Transcriptional regulation of thioredoxin reductase 1 expression by cadmium in vascular endothelial cells: role of NF-E2-related factor-2, J. Cell. Physiol. 203 (3) (2005) 529–537.
[9] Z. Touat-Hamici, et al., Selective up-regulation of human selenoproteins in response to oxidative stress, J. Biol. Chem. 289 (21) (2014) 14750–14761.
[10] M.C. Linder, M. Hazegh-Azam, Copper biochemistry and molecular biology, Am. J. Clin. Nutr. 63 (5) (1996) 797S–811S.
[11] B. Halliwell, J.M. Gutteridge, Oxygen toxicity, oxygen radicals, transition metals and disease, Biochem. J. 219 (1) (1984) 1–14.
[12] Y. Hatori, S. Lutsenko, An expanding range of functions for the copper chaperone/antioxidant protein Atox1, Antioxidants Redox Signal. 19 (9) (2013) 945–957.
[13] B. Zhou, J. Gitschier, hCTR1: a human gene for copper uptake identified by complementation in yeast, Proc. Natl. Acad. Sci. U. S. A. 94 (14) (1997) 7481–7486.
[14] P.V. van den Berghe, et al., Human copper transporter 2 is localized in late endosomes and lysosomes and facilitates cellular copper uptake, Biochem. J. 407 (1) (2007) 49–59.
[15] M. Arredondo, et al., DMT1, a physiologically relevant apical Cu1+ transporter of intestinal cells, Am. J. Physiol. Cell Physiol. 284 (6) (2003) C1525–C1530.
[16] A.C. Illing, et al., Substrate profile and metal-ion selectivity of human divalent metal-ion transporter-1, J. Biol. Chem. 287 (36) (2012) 30485–30496.
[17] H. Tapiero, D.M. Townsend, K.D. Tew, Trace elements in human physiology and pathology, *Copper*. Biomed Pharmacother 57 (9) (2003) 386–398.
[18] V.C. Culotta, et al., The copper chaperone for superoxide dismutase, J. Biol. Chem. 272 (38) (1997) 23469–23472.
[19] J.R. Prohaska, M. Broderius, B. Brokate, Metallochaperone for Cu,Zn-superoxide dismutase (CCS) protein but not mRNA is higher in organs from copper-deficient mice and rats, Arch. Biochem. Biophys. 417 (2) (2003) 227–234.
[20] J.H. Freedman, M.R. Ciriolo, J. Peisach, The role of glutathione in copper metabolism and toxicity, J. Biol. Chem. 264 (10) (1989) 5598–5605.
[21] J. Jiang, et al., Contribution of glutathione and metallothioneins to protection against copper toxicity and redox cycling: quantitative analysis using MT+/+ and MT-/- mouse lung fibroblast cells, Chem. Res. Toxicol. 15 (8) (2002) 1080–1087.
[22] O.M. Steinebach, H.T. Wolterbeek, Role of cytosolic copper, metallothionein and glutathione in copper toxicity in rat hepatoma tissue culture cells, Toxicology 92 (1–3) (1994) 75–90.
[23] Y. Chen, J.T. Saari, Y.J. Kang, Weak antioxidant defenses make the heart a target for damage in copper-deficient rats, Free Radic. Biol. Med. 17 (6) (1994) 529–536.
[24] K.L. Olin, R.M. Walter, C.L. Keen, Copper deficiency affects selenoglutathione peroxidase and selenodeiodinase activities and antioxidant defense in weanling rats, Am. J. Clin. Nutr. 59 (3) (1994) 654–658.
[25] J.R. Prohaska, R.A. Sunde, K.R. Zinn, Livers from copper-deficient rats have lower glutathione peroxidase activity and mRNA levels but normal liver selenium levels, J. Nutr. Biochem. 3 (8) (1992) 429–436.
[26] L.S. Jensen, Modification of a selenium toxicity in chicks by dietary silver and copper, J. Nutr. 105 (6) (1975) 769–775.
[27] R.L. Davis, J.E. Spallholz, B.C. Pence, Inhibition of selenite-induced cytotoxicity and apoptosis in human colonic carcinoma (HT-29) cells by copper, Nutr. Canc. 32 (3) (1998) 181–189.
[28] K. Silva, J. Sundberg, H. Hedrich, The Laboratory Mouse, 2012.
[29] K. Lossow, et al., Aging affects sex- and organ-specific trace element profiles in mice, Aging (Albany NY) 12 (13) (2020) 13762–13790.
[30] M. Böcher, et al., Synthesis of mono- and bifunctional peptide-dextran conjugates for the immobilization of peptide antigens on ELISA plates: properties and application, J. Immunol. Methods 208 (2) (1997) 191–202.
[31] S. Florian, et al., Loss of GPx2 increases apoptosis, mitosis, and GPx1 expression in the intestine of mice, Free Radic. Biol. Med. 49 (11) (2010) 1694–1702.
[32] S. Krehl, et al., Glutathione peroxidase-2 and selenium decreased inflammation and tumors in a mouse model of inflammation-associated carcinogenesis whereas sulforaphane effects differed with selenium supply, Carcinogenesis 33 (3) (2012) 620–628.
[33] M. Müller, et al., Nrf2 target genes are induced under marginal selenium-deficiency, Genes Nutr. 5 (4) (2010) 297–307.
[34] J.R. Winther, C. Thorpe, Quantification of thiols and disulfides, Biochim. Biophys. Acta 1840 (2) (2014) 838–846.
[35] M.O. Song, J. Li, J.H. Freedman, Physiological and toxicological transcriptome changes in HepG2 cells exposed to copper, Physiol. Genom. 38 (3) (2009) 386–401.
[36] X. Ding, H. Xie, Y.J. Kang, The significance of copper chelators in clinical and experimental application, J. Nutr. Biochem. 22 (4) (2011) 301–310.
[37] M. Schwarz, et al., Crosstalk of Nrf2 with the trace elements selenium, iron, zinc, and copper, Nutrients 11 (9) (2019).
[38] C. Lennicke, et al., Individual effects of different selenocompounds on the hepatic proteome and energy metabolism of mice, Biochim. Biophys. Acta Gen. Subj. 1861 (1 Pt A) (2017) 3323–3334.

[39] K.T. Suzuki, et al., Roles of metallothionein in copper homeostasis: responses to Cu-deficient diets in mice, J. Inorg. Biochem. 88 (2) (2002) 173–182.
[40] J. Chung, J.R. Prohaska, M. Wessling-Resnick, Ferroportin-1 is not upregulated in copper-deficient mice, J. Nutr. 134 (3) (2004) 517–521.
[41] K.G. Allen, et al., Copper deficiency and tissue glutathione concentration in the rat, Proc. Soc. Exp. Biol. Med. 187 (1) (1988) 38–43.
[42] H. Chun, et al., Organ-specific regulation of ATP7A abundance is coordinated with systemic copper homeostasis, Sci. Rep. 7 (1) (2017) 12001.
[43] Y. Nose, B.E. Kim, D.J. Thiele, Ctr1 drives intestinal copper absorption and is essential for growth, iron metabolism, and neonatal cardiac function, Cell Metabol. 4 (3) (2006) 235–244.
[44] D. Huster, et al., Consequences of copper accumulation in the livers of the Atp7b-/- (Wilson disease gene) knockout mice, Am. J. Pathol. 168 (2) (2006) 423–434.
[45] J.R. Turnlund, Stable isotope studies of the effect of dietary copper on copper absorption and excretion, Adv. Exp. Med. Biol. 258 (1989) 21–28.
[46] W. Buckley, et al., Effect of selenium supplementation on copper metabolism in dairy cows, Can. J. Anim. Sci. 66 (4) (1986) 1009–1018.
[47] M.S. Fehrs, et al., Effect of high but nontoxic dietary intake of copper and selenium on metabolism in calves, J. Dairy Sci. 64 (8) (1981) 1700–1706.
[48] J.L. Burkhead, et al., Elevated copper remodels hepatic RNA processing machinery in the mouse model of Wilson's disease, J. Mol. Biol. 406 (1) (2011) 44–58.
[49] J. Van Ryssen, P. Van Malsen, F. Hartmann, Contribution of dietary sulphur to the interaction between selenium and copper in sheep, J. Agric. Sci. 130 (1) (1998) 107–114.
[50] R.A. Sunde, et al., Selenium status highly regulates selenoprotein mRNA levels for only a subset of the selenoproteins in the selenoproteome, Biosci. Rep. 29 (5) (2009) 329–338.
[51] A. Kipp, et al., Four selenoproteins, protein biosynthesis, and Wnt signalling are particularly sensitive to limited selenium intake in mouse colon, Mol. Nutr. Food Res. 53 (12) (2009) 1561–1572.
[52] N.M. Tassabehji, J.W. VanLandingham, C.W. Levenson, Copper alters the conformation and transcriptional activity of the tumor suppressor protein p53 in human Hep G2 cells, Exp. Biol. Med. 230 (10) (2005) 699–708.
[53] J.W. Vanlandingham, et al., Expression profiling of p53-target genes in copper-mediated neuronal apoptosis, NeuroMolecular Med. 7 (4) (2005) 311–324.
[54] M. Tan, et al., Transcriptional activation of the human glutathione peroxidase promoter by p53, J. Biol. Chem. 274 (17) (1999) 12061–12066.
[55] S.P. Hussain, et al., p53-induced up-regulation of MnSOD and GPx but not catalase increases oxidative stress and apoptosis, Canc. Res. 64 (7) (2004) 2350–2356.
[56] Z.R. Stoytcheva, et al., Metal transcription factor-1 regulation via MREs in the transcribed regions of selenoprotein H and other metal-responsive genes, Biochim. Biophys. Acta 1800 (3) (2010) 416–424.
[57] R. Heuchel, et al., The transcription factor MTF-1 is essential for basal and heavy metal-induced metallothionein gene expression, EMBO J. 13 (12) (1994) 2870–2875.
[58] K. Renko, et al., Down-regulation of the hepatic selenoprotein biosynthesis machinery impairs selenium metabolism during the acute phase response in mice, Faseb. J. 23 (6) (2009) 1758–1765.
[59] C. Vindry, T. Ohlmann, L. Chavatte, Translation regulation of mammalian selenoproteins, Biochim. Biophys. Acta Gen. Subj. 1862 (11) (2018) 2480–2492.
[60] R. Tobe, et al., High error rates in selenocysteine insertion in mammalian cells treated with the antibiotic doxycycline, chloramphenicol, or geneticin, J. Biol. Chem. 288 (21) (2013) 14709–14715.
[61] X.M. Xu, et al., Targeted insertion of cysteine by decoding UGA codons with mammalian selenocysteine machinery, Proc. Natl. Acad. Sci. U. S. A. 107 (50) (2010) 21430–21434.
[62] A.A. Turanov, et al., Regulation of selenocysteine content of human selenoprotein P by dietary selenium and insertion of cysteine in place of selenocysteine, PLoS One 10 (10) (2015), e0140353.
[63] J. Lu, et al., Penultimate selenocysteine residue replaced by cysteine in thioredoxin reductase from selenium-deficient rat liver, Faseb. J. 23 (8) (2009) 2394–2402.
[64] A. Bhattacharjee, K. Chakraborty, A. Shukla, Cellular copper homeostasis: current concepts on its interplay with glutathione homeostasis and its implication in physiology and human diseases, Metallomics 9 (10) (2017) 1376–1388.
[65] I. Jimenez, et al., Chronic exposure of HepG2 cells to excess copper results in depletion of glutathione and induction of metallothionein, Toxicol. Vitro 16 (2) (2002) 167–175.
[66] H. Yamamoto, et al., Mechanism of enhanced lipid peroxidation in the liver of Long-Evans cinnamon (LEC) rats, Arch. Toxicol. 73 (8–9) (1999) 457–464.
[67] J.O. Ossola, M.D. Groppa, M.L. Tomaro, Relationship between oxidative stress and heme oxygenase induction by copper sulfate, Arch. Biochem. Biophys. 337 (2) (1997) 332–337.
[68] H. Nagasaka, et al., Relationship between oxidative stress and antioxidant systems in the liver of patients with Wilson disease: hepatic manifestation in Wilson disease as a consequence of augmented oxidative stress, Pediatr. Res. 60 (4) (2006) 472–477.
[69] G. Gromadzka, et al., Treatment with D-penicillamine or zinc sulphate affects copper metabolism and improves but not normalizes antioxidant capacity parameters in Wilson disease, Biometals 27 (1) (2014) 207–215.
[70] V. Gandin, A.P. Fernandes, Metal- and semimetal-containing inhibitors of thioredoxin reductase as anticancer agents, Molecules 20 (7) (2015) 12732–12756.
[71] A.R. Mufti, et al., XIAP Is a copper binding protein deregulated in Wilson's disease and other copper toxicosis disorders, Mol. Cell 21 (6) (2006) 775–785.
[72] F. Bulcke, et al., Modulation of copper accumulation and copper-induced toxicity by antioxidants and copper chelators in cultured primary brain astrocytes, J. Trace Elem. Med. Biol. 32 (2015) 168–176.
[73] H. Wei, et al., Copper chelation by tetrathiomolybdate inhibits lipopolysaccharide-induced inflammatory responses in vivo, Am. J. Physiol. Heart Circ. Physiol. 301 (3) (2011) H712–H720.
[74] N. Goto, et al., Hydrogen sulfide increases copper-dependent neurotoxicity via intracellular copper accumulation, Metallomics 12 (6) (2020) 868–875.
[75] S. Olusi, et al., Serum copper levels and not zinc are positively associated with serum leptin concentrations in the healthy adult population, Biol. Trace Elem. Res. 91 (2) (2003) 137–144.
[76] J. Baudry, et al., Changes of trace element status during aging: results of the EPIC-Potsdam cohort study, Eur. J. Nutr. (2019) 1–14.
[77] S. Kumru, et al., Comparison of serum copper, zinc, calcium, and magnesium levels in preeclamptic and healthy pregnant women, Biol. Trace Elem. Res. 94 (2) (2003) 105–112.
[78] R.A. Lewis, et al., Hypercupremia associated with a monoclonal immunoglobulin, J. Lab. Clin. Med. 88 (3) (1976) 375–388.
[79] S. Goldfischer, H. Popper, I. Sternlieb, The significance of variations in the distribution of copper in liver disease, Am. J. Pathol. 99 (3) (1980) 715–730.
[80] Q. Sun, et al., Selenium and copper as biomarkers for pulmonary arterial hypertension in systemic sclerosis, Nutrients 12 (6) (2020).
[81] P. Ozturk, E. Belge Kurutas, A. Ataseven, Copper/zinc and copper/selenium ratios, and oxidative stress as biochemical markers in recurrent aphthous stomatitis, J. Trace Elem. Med. Biol. 27 (4) (2013) 312–316.